

Dielectric Properties and Crystal Structure of $(\text{Mg}_{0.95}\text{Ni}_{0.05})_4(\text{Nb}_{1-x}\text{Ta}_x)_2\text{O}_9$ Ceramics

Bing-Jing Li¹, Sih-Yin Wang¹ and Yuan-Bin Chen^{2*}

¹Department of Electrical Engineering, National Cheng Kung University, 1 University Rd., Tainan 70101, Taiwan

²Department of Engineering and Management of Advanced Technology, Chang Jung Christian University, Tainan 71101, Taiwan

Abstract

The microstructure of $(\text{Mg}_{0.95}\text{Ni}_{0.05})_4(\text{Nb}_{1-x}\text{Ta}_x)_2\text{O}_9$ is analyzed using X-ray diffractometry and scanning electron microscopy. The Qxf values of $(\text{Mg}_{0.95}\text{Ni}_{0.05})_4(\text{Nb}_{1-x}\text{Ta}_x)_2\text{O}_9$ increases with increasing sintering temperature; and then up to a temperature of 1375°C significantly decreased. The maximum values of the electric permittivity and the quality factor (Qxf) can be obtained 12.76 and 442,000 GHz is obtained for $(\text{Mg}_{0.95}\text{Ni}_{0.05})_4(\text{Nb}_{1-x}\text{Ta}_x)_2\text{O}_9$ sintered at 1375°C for 4 h. The temperature coefficient of resonant frequency (τ_f) measured for $(\text{Mg}_{0.95}\text{Ni}_{0.05})_4(\text{Nb}_{1-x}\text{Ta}_x)_2\text{O}_9$ is -54 ppm/°C.

Keywords: Crystal structure; X-ray diffractometry; Wireless communication

Introduction

The rapid growth of recent wireless communication systems led to an increasing demand for small-scale high-frequency resonators, filters and antennas capable of operating in the GHz range [1-3]. The unique electrical properties of ceramic dielectric resonators have revolutionized the microwave-based wireless communications industry by reducing the size and cost of filter and oscillator components in circuit systems [4,5]. At the same time, in order to work with high efficiency and stability, many researches have been focusing on developing new dielectric materials with a high quality factor ($Q \times f$) and a near-zero temperature coefficient of resonant frequency (τ_f) for use as dielectric resonator and microwave device substrate [6-8].

$\text{Mg}_4\text{Nb}_2\text{O}_9$ has been found to have an electric permittivity of 12.4, a temperature coefficient of resonant frequency τ_f of ~ -70 ppm/°C and a high Qxf of $\sim 194,000$ GHz [9]. However, a sintering temperature of as high as 1350-1400°C and a sintering time of 10 h are required. The high sintering temperature limits the application of these ceramics will limit its applications for practical cases. In addition, the Qxf value needs to be increased for high-frequency applications.

In this paper, the Ni^{2+} are doped into $\text{Mg}_4\text{Nb}_2\text{O}_9$ to form $(\text{Mg}_{0.95}\text{Ni}_{0.05})_4\text{Nb}_2\text{O}_9$. Because the ionic radius of Mg^{2+} (0.78 Å) is similar to those of Ni^{2+} (0.69 Å). Ni^{2+} substitutes Mg^{2+} to improve the quality factor. The Ta^{5+} substitution content Nb^{5+} to formed $(\text{Mg}_{0.95}\text{Ni}_{0.05})_4(\text{Nb}_{1-x}\text{Ta}_x)_2\text{O}_9$, we discovered it improved the microwave dielectric properties. The effect of Ta^{5+} substituting Nb^{5+} on the structure and microwave dielectric properties of $(\text{Mg}_{0.95}\text{Ni}_{0.05})_4(\text{Nb}_{1-x}\text{Ta}_x)_2\text{O}_9$ is investigated.

Experimental Procedures

$(\text{Mg}_{0.95}\text{Ni}_{0.05})_4(\text{Nb}_{1-x}\text{Ta}_x)_2\text{O}_9$ powders were prepared using the solid-state reaction method by mixing individual high-purity oxides MgO, NiO, Ta_2O_5 and Nb_2O_5 . The starting materials were stoichiometrically weighed after MgO was sintered at 800°C for 6 h to remove moisture content and carbonates. The powders were then dry-mixed with an agate mortar and pestle and subsequently wet-mixed using distilled water. The calcination temperature was varied in the range of 900 to 1100°C. The calcined powder with the organic binder polyvinyl alcohol was pressed into pellets using a uniaxial press. The binder was then evaporated at 650°C for 12 h. Sintering was carried out at 1250-1425°C for 4 h. The powder and bulk X-ray diffraction (XRD, Rigaku D/Max

III.V) patterns were collected using Cu K α radiation (at 30 kV and 20 mA) and a graphite monochromator in the 2θ range of 20 to 60°C. The microstructural observations and analysis of the sintered surface were performed by a scanning electron microscopy (SEM, Philips XL-40FEG).

The bulk densities of the sintered pellets were measured using the Archimedes method. Microwave dielectric properties such as the electric permittivity and unloaded Q were measured at 6-12 GHz using the post-resonant method as suggested by Hakki and Coleman [10]. This method uses parallel conducting plates and coaxial probes on TE_{011} mode, where TE means transverse electric waves, the first two subscript integers denote the wave guide mode, and the third integer denotes the order of resonance in an increasing set of discrete resonant lengths. The temperature coefficient of resonant frequency was measured in the temperature range of 20-80°C. A system that combines an HP8757D network analyzer and an HP8350B sweep oscillator were employed in the measurement.

Results and Discussion

Microwave dielectric properties of $(\text{Mg}_{0.95}\text{Ni}_{0.05})_4(\text{Nb}_{1-x}\text{Ta}_x)_2\text{O}_9$ ($x=0-1.0$) ceramic system sintered at various temperatures for 4 h are illustrated in Table 1 and Figure 1 shown the room-temperature X-ray diffraction (XRD) patterns recorded from the $(\text{Mg}_{0.95}\text{Ni}_{0.05})_4(\text{Nb}_{1-x}\text{Ta}_x)_2\text{O}_9$ ($x=0-1.0$) ceramics sintered at 1375°C for 4 h. The single trigonal-structured $(\text{Mg}_{0.95}\text{Ni}_{0.05})_4(\text{Nb}_{1-x}\text{Ta}_x)_2\text{O}_9$ ($x=0-1.0$), belonging to the space group P3c1 (165), was identified throughout the entire tested range. The position and relative intensity of the XRD peaks varied slightly, implying that the compound tends to form a continuous solid solution. In order to confirming the formation of solid solution, the lattice parameters of $(\text{Mg}_{0.95}\text{Ni}_{0.05})_4(\text{Nb}_{1-x}\text{Ta}_x)_2\text{O}_9$ ($x=1$) ceramics

*Corresponding author: Yuan-Bin Chen, Department of Engineering and Management of Advanced Technology, Chang Jung Christian University, Tainan 71101, Taiwan, Tel: +886-6-2785123-6112; E-mail: cubnck@yahoo.com.tw

Received September 11, 2014; Accepted September 23, 2014; Published September 29, 2014

Citation: Li BJ, Wang SY, Chen YB (2014) Dielectric Properties and Crystal Structure of $(\text{Mg}_{0.95}\text{Ni}_{0.05})_4(\text{Nb}_{1-x}\text{Ta}_x)_2\text{O}_9$ Ceramics. J Material Sci Eng 3: 140. doi:10.4172/2169-0022.1000140

Copyright: © 2014 Bing-Jing Li, et al. This is an open-access article distributed under the terms of the Creative Commons Attribution License, which permits unrestricted use, distribution, and reproduction in any medium, provided the original author and source are credited.

X value	Bulk density (g/cm ³)	Relative density (%)	ϵ_r	$Q \times f$ (GHz)	τ_f (ppm/°C)
0	4.34	97.17	13.84	226,403	-63.98
0.3	4.85	96.85	13.61	231,913	-60.41
0.5	5.18	96.40	13.31	255,577	-59.10
0.7	5.57	97.20	12.91	281,344	-56.88
1	6.15	97.66	12.76	442,092	-55.63

Table 1: The microwave dielectric properties of $(Mg_{0.95}Ni_{0.05})_4(Nb_{1-x}Ta_x)_2O_9$.

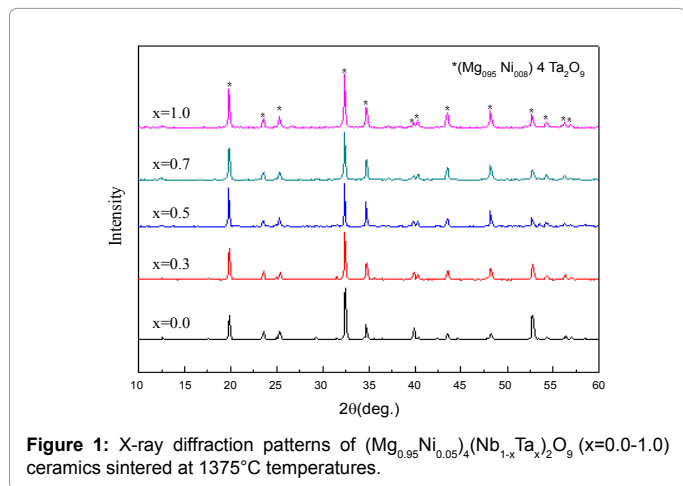


Figure 1: X-ray diffraction patterns of $(Mg_{0.95}Ni_{0.05})_4(Nb_{1-x}Ta_x)_2O_9$ ($x=0.0-1.0$) ceramics sintered at 1375°C temperatures.

sintered at various temperatures XRD pattern shown in Figure 2. It is also belonging to the space group P3c1 (165) and the single trigonal-structured without any secondary phase.

SEM photographs of $(Mg_{0.95}Ni_{0.05})_4(Nb_{1-x}Ta_x)_2O_9$ ($x=1$) ceramics sintered at various temperatures for 4 h are shown in Figure 3. The grain size increases with increasing sintering temperature. The grain size growth the most uniform sintered at 1375°C and obtained the best microwave dielectric properties as shown in Figure 4, however sinter above the 1375°C, the grain over-sintering.

The relative density and electric permittivity of $(Mg_{0.95}Ni_{0.05})_4(Nb_{1-x}Ta_x)_2O_9$ ceramics as functions of sintering temperature are shown in Figures 5 and 6. Note that the relative density initially increased with increasing sintering temperature, reaching its maximum at 1325°C ($<0x<0.03$), with increasing more Ta⁵⁺ content and the saturated relative density sintering at 1375°C ($x=1$) and then relative density decreased sintering at high temperature. The relative density of all the specimens was high above 94% of the theoretical density. The relative density increased with increasing sintering temperature due to increased Ta⁵⁺ content at higher sintering temperature. The increase in relative density mainly resulted from grain growth as, shown in from Figure 3.

The dielectric properties of $(Mg_{0.95}Ni_{0.05})_4(Nb_{1-x}Ta_x)_2O_9$ are shown in Figure 6. With the x value was increased from 0. to 1, the electric permittivity decreased from 13.84 ($x=0$ sintered at 1225°C) to 12.76 ($x=1$ sintered at 1375°C). The influence of Ta substitution for Nb on the electric permittivity and quality factor of $(Mg_{0.95}Ni_{0.05})_4(Nb_{1-x}Ta_x)_2O_9$ for various values of x is shown in Figure 5. The electric permittivity values of $(Mg_{0.95}Ni_{0.05})_4(Nb_{1-x}Ta_x)_2O_9$ slightly decreased with increasing value of x; These values for $(Mg_{0.95}Ni_{0.05})_4(Nb_{1-x}Ta_x)_2O_9$ are very similar to those for Al₂O₃ and SAT [11,12].

The electric permittivity of microwave dielectric ceramics is

affected by ionic polarizability [13]; The electric permittivity values of $(Mg_{0.95}Ni_{0.05})_4(Nb_{1-x}Ta_x)_2O_9$ decreased with increasing Ta⁵⁺ substitution for Nb⁵⁺. Similar result was reported for SAN and SAT; Guo et al. [14] suggest that the differences between SAT and SAN are not unique to these two materials, but are common to all Nb⁵⁺ compounds and their analogous Ta compounds. It is insufficient to explain the reason for those differences by, for instance, simply considering the bonding strength (as they have the same valence and coordination numbers), or on the basis of available ionic polarizability data ($\alpha_i^{Ta5+} = 4.73 \text{ \AA}^3$ and $\alpha_i^{Nb5+} = 3.97 \text{ \AA}^3$ that would predict a lesser polarizability for SAN than SAT). It seems to us that the electronic structure differences may have caused the Ta-O bonding to be less ionic in nature and somehow enhanced the bonding strength in the crystal structures of SAN and SAT may exert an influence on the decrease in the electric permittivity value. Thus, it is considered the observed ionic polarizability (α_{obs}) of $(Mg_{0.95}Ni_{0.05})_4(Nb_{1-x}Ta_x)_2O_9$ was estimated in order to clarify the effects of the Ta substitution for Nb on the ϵ_r by using the Clausius-Mosotti equation:

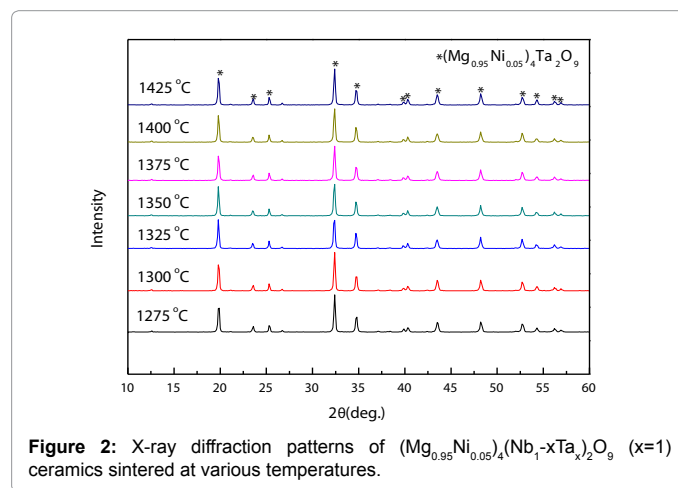


Figure 2: X-ray diffraction patterns of $(Mg_{0.95}Ni_{0.05})_4(Nb_{1-x}Ta_x)_2O_9$ ($x=1$) ceramics sintered at various temperatures.

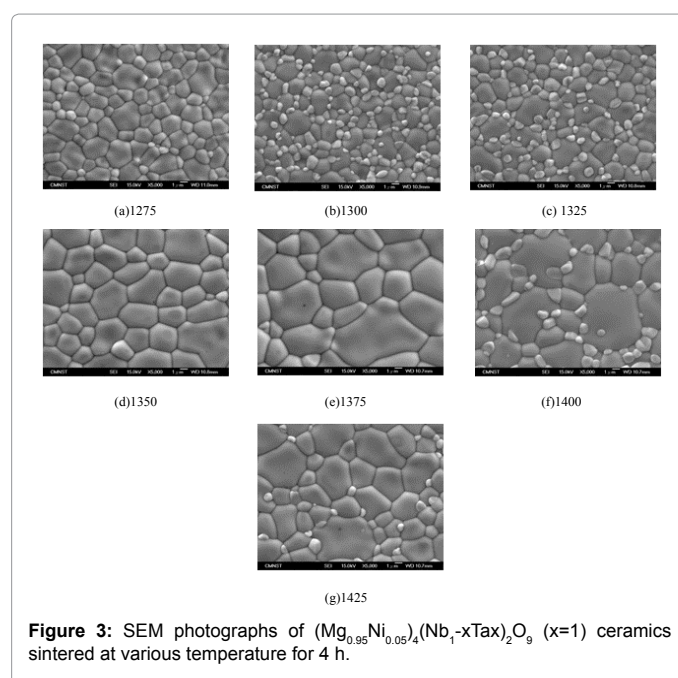


Figure 3: SEM photographs of $(Mg_{0.95}Ni_{0.05})_4(Nb_{1-x}Tax)_2O_9$ ($x=1$) ceramics sintered at various temperature for 4 h.

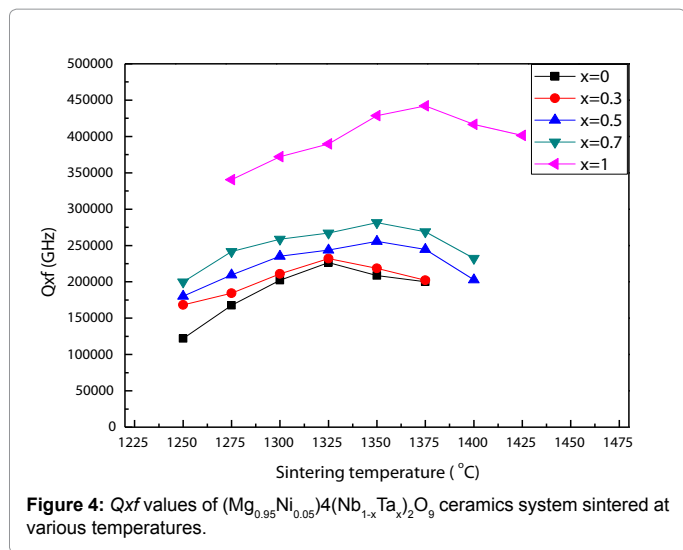


Figure 4: Qxf values of $(Mg_{0.95}Ni_{0.05})_4(Nb_{1-x}Ta_x)_2O_9$ ceramics system sintered at various temperatures.

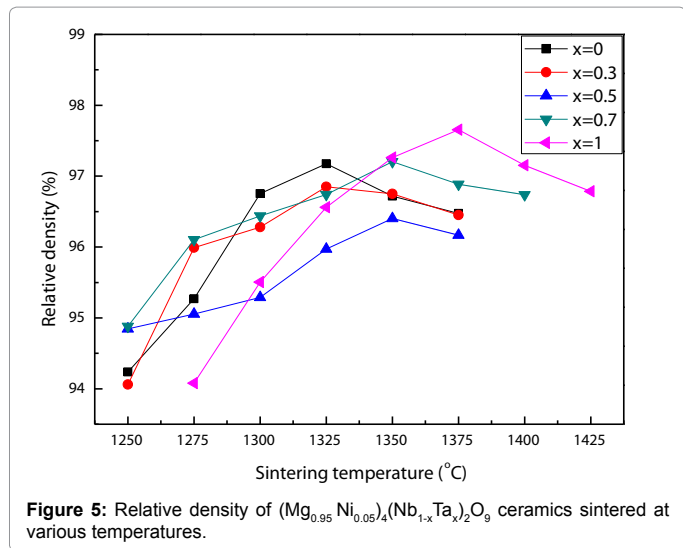


Figure 5: Relative density of $(Mg_{0.95}Ni_{0.05})_4(Nb_{1-x}Ta_x)_2O_9$ ceramics sintered at various temperatures.

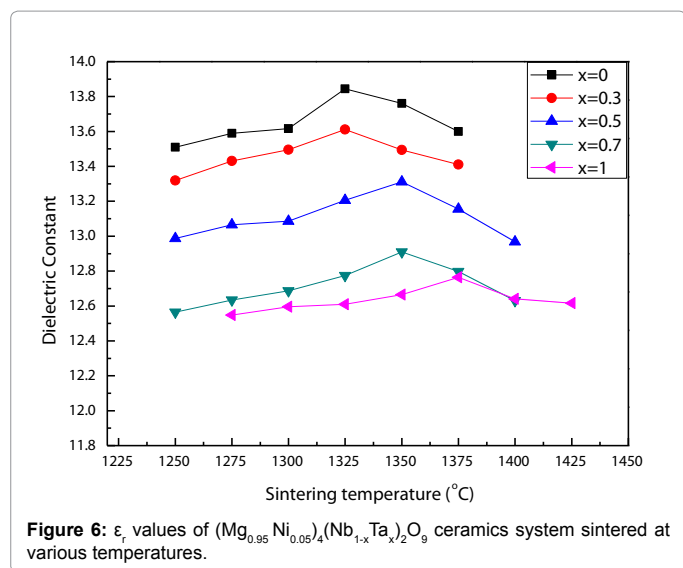


Figure 6: ϵ_r values of $(Mg_{0.95}Ni_{0.05})_4(Nb_{1-x}Ta_x)_2O_9$ ceramics system sintered at various temperatures.

$$\epsilon_r = \frac{3V_m + 8\pi\alpha_m}{3V_m - 4\pi\alpha_m} \quad (1)$$

where ϵ_r , V_m , and α_m represent the relative permittivity, molar volume, and macroscopic polarizability, respectively. Using the experimental relative permittivity data and unit-cell volume data, the macroscopic polarizability, α_m , was calculated. The theoretical polarizability data show an almost sigmoidal increase with increasing in Zn content and the unit-cell volume increasing with x . The relative permittivity increases with α_m . When the value of α_m approaches $3V_m/4\pi$, the relative permittivity increases very rapidly. It has also been reported that the macroscopic polarizability of complex systems with an ideal symmetry can be determined from the summation of the polarizability of the constituent cations:

$$\alpha_m = \sum \alpha_{(ions)} \quad (2)$$

The theoretical polarizability values (denoted as $\alpha_m(\text{theory})$) values calculated using Eq. (2) are compared with the experimental polarizability values (determined using the Clausius–Mossotti relation, Eq. (1)). It is noted that $\alpha_m(\text{exp})$ for the $(Mg_{0.95}Ni_{0.05})_4(Nb_{1-x}Ta_x)_2O_9$ end member is less than the $\alpha_m(\text{theory})$ value. Shannon [12] suggested that deviations from the additivity of ionic polarizability arise when compression or rattling of cations occurs at the structural sites as the cation sizes are varied. The lower $\alpha_m(\text{exp})$ value for $(Mg_{0.95}Ni_{0.05})_4(Nb_{1-x}Ta_x)_2O_9$ may thus be due to compression effects caused by the large difference between the ionic polarizabilities of Nb^{5+} and Ta^{5+} . This correlation agrees with the harmonic-oscillator model [14]. The unique relationship between permittivity and internal lattice stress is analogous to the reversible changes in permittivity with applied external stress reported by Steiner et al. [15].

Figure 4 shows the Qxf value of $(Mg_{0.95}Ni_{0.05})_4(Nb_{1-x}Ta_x)_2O_9$ ceramics at various sintering temperatures as a function of the x value. The Qxf value increased with increasing Ta^{5+} content and sintering temperature. Many factors can affect the microwave dielectric loss of dielectric resonators, such as the lattice vibration modes, pores, and secondary phases. Generally, a larger grain size, i.e., a smaller grain boundary, indicates a reduction in lattice imperfection and thus reduced dielectric loss. When the x value was increased from 0 to 1, the Qxf values of $(Mg_{0.95}Ni_{0.05})_4(Nb_{1-x}Ta_x)_2O_9$ increased dramatically from 226,000GHz ($x=0 \sim 1325^\circ\text{C}$) to 442,000GHz ($x=1 \sim 1375^\circ\text{C}$) GHz; which is comparable to that of Al_2O_3 . Relative density also plays an important role in controlling dielectric loss, as has been shown for other microwave dielectric materials. As well known, factors that influence the dielectric Q fall into two categories: intrinsic and extrinsic. The former is due to the interaction between polar phonon vibration with the microwave electric field in crystals, while the latter includes order-disorder transformation, pore density, grain size, oxygen vacancy, and impurity phases in ceramics. The intrinsic Q sets the upper limit value for a pure defect-free single crystal and can be quantitatively described by the well-known classical damped oscillator model in microwave frequency range. In this model, when employing one-phonon absorption approximation, a roughly reciprocal relationship between Qxf and the ϵ_r could be obtained as

$$Qxf \propto \epsilon_r^{-1} \quad (3)$$

where the frequency f should be limited to the vicinity of the phonon engine frequencies, of the order of 10^{12} Hz at room temperature, to make the estimation valid. However, a series of experiments evidenced that the extrapolation of Eq. (2) from microwave frequencies down to megawatt frequencies (1-4 magnitude orders below the optical phonon

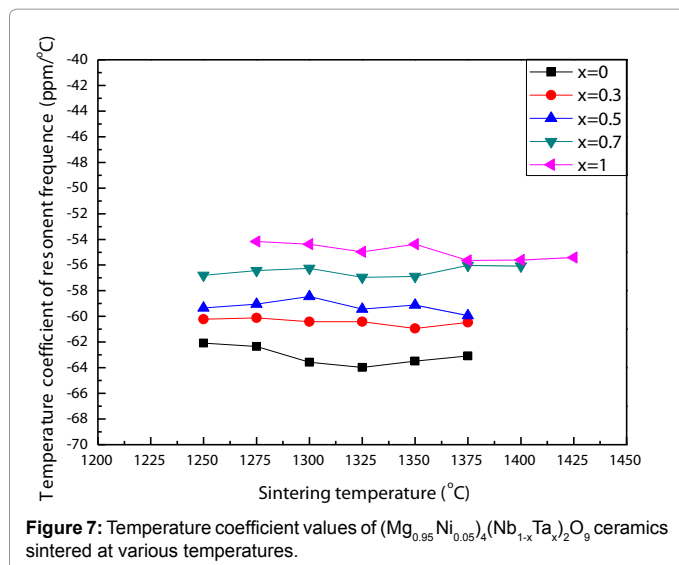


Figure 7: Temperature coefficient values of $(Mg_{0.95}Ni_{0.05})_4(Nb_{1-x}Ta_x)_2O_9$ ceramics sintered at various temperatures.

engine frequency) at room temperature could also give a satisfying magnitude order of dielectric Q for well processed ceramics. The result, however, showed that the dependence of Qxf on ϵ_r only yielded $Qxf \propto \epsilon_r^{-0.6}$, indicating a rather smoother increasing rate of Qxf value with ϵ_r compared with Eq. (2). The most probable reason for this phenomenon could be associated with the extrinsic origins. As acknowledged by many authors, the porosity in dielectrics had deleterious effects on dielectric Qxf values, whose influencing degree, however, varied with different dielectrics. For low dielectric Qxf ceramics with 10^3 GHz magnitude order, the effect of porosity on dielectric Q could be described as

$$Q = Q_0(1 - 1.5P) \quad (4)$$

where Q_0 was the intrinsic dielectric Q measured by microwave reflective spectrum and P was the porosity. However, as for high Qxf ceramics with 10^5 - 10^6 GHz magnitude order such as polycrystalline Al_2O_3 ceramic, even a small amount of porosity would considerably reduce the dielectric Q by

$$\frac{1}{Q} = (1 - P) \frac{1}{Q_0} + A'P \left(\frac{P}{1 - P} \right)^{2/3} \quad (5)$$

The τ_f values of $(Mg_{0.95}Ni_{0.05})_4(Nb_{1-x}Ta_x)_2O_9$ ranged from -54 to -66 ppm/°C, as shown in Figure 7. The temperature coefficient of resonant frequency, τ_f (TCF), could be defined as following:

$$TCF = -\alpha_1 - \frac{1}{2}\tau_\epsilon \quad (6)$$

Where α_1 is the linear thermal expansion coefficient and τ_ϵ is the temperature coefficient of permittivity. Using the Clausius-Mosotti equation, Bosman and Havinga [16] derived the following expression for τ_ϵ at a constant pressure:

$$\tau_\epsilon = \frac{1}{\epsilon} \left(\frac{\partial \epsilon}{\partial T} \right)_p = \frac{(\epsilon - 1)(\epsilon + 2)}{\epsilon} (A + B + C) = \left(\epsilon - \frac{2}{\epsilon} + 1 \right) (A + B + C)$$

$$A = \frac{1}{3V} \left(\frac{\partial V}{\partial T} \right)_p$$

$$B = \frac{1}{3\alpha_m} \left(\frac{\partial \alpha_m}{\partial V} \right)_T \left(\frac{\partial V}{\partial T} \right)_p$$

$$C = \frac{1}{3\alpha_m} \left(\frac{\partial \alpha_m}{\partial T} \right)_p$$

The $(A+B+C)$ value can be extrapolated from Eq. (1) as -10.95 ppm/°C. When the $(A+B+C)$ value is negative, TCF value increases

with permittivity. When the $(A+B+C)$ value is positive, the TCF value decreases permittivity. Usually, the absolute value of TCF increases with permittivity. The sum of the A and B terms is approximately 6 ± 1 ppm/°C. For term C, the suggested value is in the range of -1 to -10 ppm/°C. The term C represents the direct dependence of the polarizability on temperature.

Conclusions

The microwave dielectric properties of the $(Mg_{0.95}Ni_{0.05})_4(Nb_{1-x}Ta_x)_2O_9$ solid solutions were investigated. The quality factors of the $(Mg_{0.95}Ni_{0.05})_4(Nb_{1-x}Ta_x)_2O_9$ solid solutions was increased by Nb^{5+} substituting for Ta^{5+} and Ni^{2+} substituting for Mg^{2+} . When x was increased from 0 to 1, the Qxf value of $(Mg_{0.95}Ni_{0.05})_4(Nb_{1-x}Ta_x)_2O_9$ increased dramatically from 226,000GHz ($x=0 \sim 1325^\circ C$) to 442,000GHz ($x=1 \sim 1375^\circ C$) GHz. So $(Mg_{0.95}Zn_{0.05}Co_{0.05})_4(Nb_{0.1}Ta_{0.9})_2O_9$ improved the microwave dielectric properties and decreased the sintering temperatures compared to pure $Mg_4Nb_2O_9$. The $(Mg_{0.95}Ni_{0.05})_4(Nb_{1-x}Ta_x)_2O_9$ compound exhibits a good combination of $\epsilon_r \sim 12.76$, $Qxf \sim 442,000$ GHz, and $\tau_f \sim -55.63$ ppm/°C after sintering at $1375^\circ C$ for 4 h. The proposed dielectric, having extremely low loss had made is a very promising material for microwave and millimeter-wave applications.

Acknowledgement

This work was supported by the National Science Council of Taiwan.

References

- Wu SP, Chen DF, Mei YX, Ma Q (2012) Synthesis and microwave dielectric properties of $Ca_3SnSi_2O_9$ ceramics. J Alloys Compd 521: 8-11.
- Bian JJ, Wu JY, Wang L (2012) Structural evolution, sintering behavior and microwave dielectric properties of $(1-x)Li_3NbO_4 \cdot xLiF$ ($0 \leq x \leq 0.9$). J Eur Ceram Soc 32: 1251-1259.
- Chen YB (2011) A simple catalyst-free route for large-scale synthesis of SiC nanowires. J Alloys Compd 509: 6884-6887.
- Chen YC (2012) Elucidating the microwave dielectric properties of $(Mg_{1-x}Zn_x)_2SnO_4$ ceramics. J Alloys Compd 527: 84-89.
- Huang CL, Huang SH (2012) Low-loss microwave dielectric ceramics in the $(Co_{1-x}Zn_x)TiO_3$ ($x = 0-0.1$) system. J Alloys Compd 515: 8-11.
- Chen YB (2012) Dielectric properties and crystal structure of Mg_2TiO_4 ceramics substituting Mg^{2+} with Zn^{2+} and Co^{2+} . J Alloys Compd 513: 481-486.
- Parida S, Rout SK, Subramanian V, Barhai PK, Gupta N, et al. (2012) Structural, microwave dielectric properties and dielectric resonator antenna studies of $Sr(Zr_{1-x}Ti_x)O_3$ ceramics. J Alloys Compd 528: 126-134.
- Zhang P, Hua Y, Xia W, Li L (2012) Effect of H_2BO_3 on the low temperature sintering and microwave dielectric properties of $Li_2ZnTi_3O_9$ ceramics. J Alloys Compd 534: 9-12.
- Dou G, Zhou D, Guo M, Gong S (2012) Low-temperature sintered Zn_2SiO_4 - $CaTiO_3$ ceramics with near-zero temperature coefficient of resonant frequency. J Alloys Compd 513: 466-473.
- Yoshida A, Ogawa H, Kan A, Ishihar S, Higashida Y (2004) Influence of Zn and Ni substitutions for Mg on dielectric properties of $(Mg_{4-x}M_x)(Nb_{2-y}Sb_y)O_9$ ($M=Zn$ and Ni) solid solutions. J Eur Ceram Soc 24: 1765-1768.
- Kagata H, Inoue T, Kato J, Kameyama I (1992) Low-Fire Bismuth-Based Dielectric Ceramics for Microwave Use. Jpn J Appl Phys 31: 3152.
- Guo R, Bhalla AS, Sheen J, Ainger FW, Erdei S, et al. (1995) Strontium aluminum tantalum oxide and strontium aluminum niobium oxide as potential substrates for HTSC thin films. J Mater Res 10: 18-25.
- Ogawaa H, Kana A, Ishihara S, Higashidab Y (2003) Crystal structure of corundum type $Mg_4(Nb_{2-x}Ta_x)O_9$ microwave dielectric ceramics with low dielectric loss. J Eur Ceram Soc 23: 2485-2488.
- Shannon RD (1993) Dielectric polarizabilities of ions in oxides and fluorides. J Appl Phys 73: 348.

15. Glazer AM (1972) The classification of tilted octahedra in perovskites. *Acta Crystallogr B* 28: 3384-3392.
16. Bosman AJ, Havinga EE (1963) Temperature Dependence of Dielectric Constants of Cubic Ionic Compounds. *Phys Rev* 129: 1593.